

Draft Report

**ASSESSMENT OF MODULAR METAL
BUILDING FOR BLAST LOADS**

BakerRisk Project No. 01-01272-001-05

Prepared for:
Safe Haven Enterprises, Inc.

Prepared by:
Matthew T. Edel, P.E.
Ali Sari
John Montoya

November 15, 2005



Baker Engineering and Risk Consultants, Inc.

3330 Oakwell Court, Suite 100 ♦ San Antonio, TX 78218-3024 ♦ (210) 824-5960 Fax: (210) 824-5964

Notice

Baker Engineering and Risk Consultants, Inc. (BakerRisk) made every reasonable effort to perform the work contained herein in a manner consistent with high professional standards.

The work was conducted on the basis of information made available to BakerRisk. Neither BakerRisk nor any person acting on its behalf makes any warranty or representation, expressed or implied, with respect to the accuracy, completeness, or usefulness of this information. All observations, conclusions and recommendations contained herein are relevant only to the project, and should not be applied to any other facility or operation.

Any third party use of this Report or any information or conclusions contained therein shall be at the user's sole risk. Such use shall constitute an agreement by the user to release, defend and indemnify BakerRisk from and against any and all liability in connection therewith (including any liability for special, indirect, incidental or consequential damages), regardless of how such liability may arise.

BakerRisk regards the work that it has done as being advisory in nature. The responsibility for use and implementation of the conclusions and recommendations contained herein rests entirely with the client.

EXECUTIVE SUMMARY

Baker Engineering & Risk Consultants, Inc. (BakerRisk) was contracted by Safe Haven Enterprises, Inc. (Safe Haven) to evaluate the design of their metal building unit (MBU) for blast loads in terms of structural response.

Structural damage was quantified using both single-degree-of-freedom (SDOF) and finite element analysis (FEA) models representing all of the structural components of the building for blast loads of multiple pressure-and-impulse combinations. Both methods resulted in developing pressure-impulse (P-i) curves that represent the blast loads that cause a specified damage level. P-i curves of increasing damage can be used to define building damage level (BDL) regions between each P-i curve, which are shown in Figure 1 for the MBU. Definitions of the BDLs are provided in Table 1. All structural analyses were completed in accordance with industry-accepted published methodologies^{1,2}.

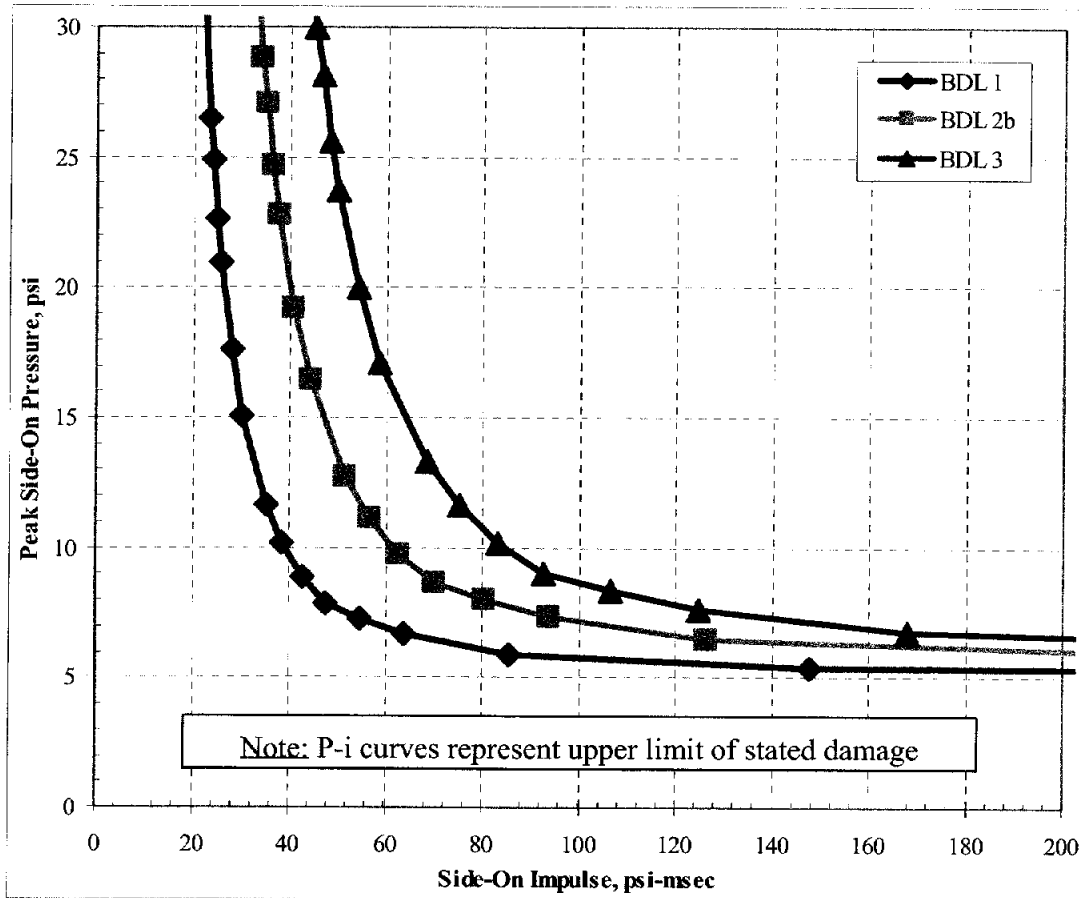


Figure 1. P-i Diagram for Building Damage to Safe Haven MBU

Table 1. BDL Definitions

Building Damage Level (BDL)	Building Consequence
1 = Minor	Onset of visible damage. Repairs are only needed for cosmetic reasons. Building is reusable following an explosion.
2a = Moderate	Localized damage. Building can be used, however repairs are required to restore integrity of structural envelope. Total cost of repairs is moderate.
2b = Heavy	Widespread damage. Building cannot be used until repaired. Total cost of repairs is significant.
3 = Major	Structure has lost integrity and may collapse due to environmental conditions (i.e., wind, snow, rain). Total cost of repairs approaches replacement cost of building.
4 = Collapse	Building fails completely. Repair is not feasible.

Table of Contents

EXECUTIVE SUMMARY	1
1. INTRODUCTION.....	1
2. METHODOLOGY	2
2.1 Blast Loads	2
2.2 Structural Analysis	3
2.2.1 SDOF Models.....	3
2.2.2 FEA Models	4
2.2.3 Pressure-Impulse Curves.....	5
3. STRUCTURAL ANALYSIS RESULTS	7
3.1 Wall and Roof Components.....	7
3.1.1 Crimped Wall Panel	7
3.1.2 Remaining Primary and Secondary Structural Components.....	10
3.1.3 Doors and Windows	12
3.2 Lateral Resisting System.....	13
3.3 Combined BDL Results.....	13
4. CONCLUSIONS.....	15
5. REFERENCES	16

APPENDIX A: DESIGN DRAWINGS

List of Tables

Table 1. BDL Definitions	ii
Table 2. Response Criteria Used to Define Damage Levels.....	4
Table 3. Component Damage Level Descriptions	4
Table 4. BDL As a Function of CDL.....	6
Table 5. Material Properties for FEA Models	8
Table 6. Free-Field P-i Curve Asymptote Values for Structural Components	11
Table 7. Free-Field P-i Curve Asymptote Values for Doors	12

List of Figures

Figure 1. P-i Diagram for Building Damage to Safe Haven MBU.....	i
Figure 2. Assumed Blast Load Characteristics.....	2
Figure 3. Equivalent Spring-Mass SDOF System	3
Figure 4. Illustration of Support Rotation Angle Used for Damage Criteria	4
Figure 5. P-i Curve Representation.....	5
Figure 6. Crimped Wall Panel FEA Model	7
Figure 7. Model Boundary Condition Display	8
Figure 8. Interior Model View.....	9
Figure 9. Crimped Panel Response for Blast Load of 40 psi and 8.75 msec.....	9
Figure 10. P-i Diagram with FEA Results for Crimped Wall Panel.....	10
Figure 11. Controlling Wall and Roof P-i Diagram	11
Figure 12. BDL P-i Diagram for MBU.....	14

1. INTRODUCTION

The Safe Haven Enterprises, Inc. (Safe Haven) metal building unit (MBU) is a 14 ft wide by 40 ft long by 9½ ft tall modular steel building designed to resist blast loading. The exterior walls of the building are constructed with ⅜-inch thick corrugated mild steel plate panels that span vertically between the eave and floor struts, which are HSS6×6×¼ and HSS12×6×¼ tube sections, respectively. There are HSS6×6×¼ columns at each corner of the building, and two additional HSS4×4×¼ columns along the long walls of the building. All wall panels, floor/roof struts, and columns are assumed to be continuously welded to one another. The floor and roof are constructed with flat ¼-inch steel plate spanning continuously over C5×6.7 joists spaced at 2 ft on center. It is assumed that the plates are continuously welded to the channels along both sides of each channel's flange. In addition, it was assumed that the roof plate is welded continuously to the eave struts along all edges. The building has two blast doors that are framed with a HSS6×6×¼ header and doorjamb. Doors consist of ¼-inch steel plates welded continuously to HSS1.5×1.5×¼ horizontal internal stiffeners. Doors also have ½-inch thick windows. All building components are welded together in a controlled shop environment. Attachments between the building and its foundation are not addressed in this study.

Baker Engineering & Risk Consultants, Inc. (BakerRisk) performed an analytical review of the MBU to determine the overall blast capacity of the building based on the design drawings in Appendix A. The review was conducted using industry-accepted analytical methods. Most of the components were analyzed assuming that they responded as independent single-degree-of-freedom (SDOF) systems. The front crimped wall panel and its supporting strut were analyzed using a finite element analysis (FEA) model. Overturning and sliding were not specifically addressed as part of this study.

2. METHODOLOGY

2.1 Blast Loads

All blast loads considered in this study were assumed to have an instantaneously-applied peak pressure followed by a linear decay to ambient pressure, as shown in Figure 2. The blast load impulse is determined as the area under the pressure-time curve. Clearing effects, a phenomenon where the reflected overpressure decays to the side-on pressure more quickly than the linear decay illustrated in Figure 2, is not included in the structural analysis. Also, any negative phase associated with the blast loads, which typically is more significant for high explosive loads, is not included in the structural analysis. More discussion is provided in Section 3.3 regarding considerations for clearing effects and negative phase loading.

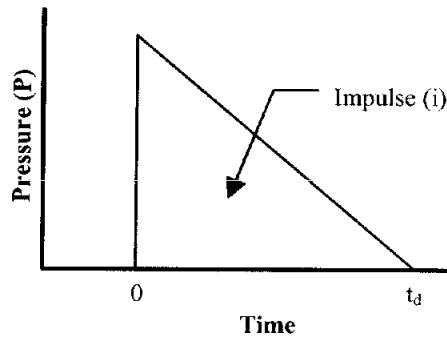


Figure 2. Assumed Blast Load Characteristics

The blast load capacities for various structural components were calculated by using the appropriate reflection factors to determine the equivalent free-field, or side-on pressures and impulses. The relationship between the reflected and side-on pressure is given in Equation 1³.

$$\frac{P_r}{P_o} = \frac{2P_s}{P_o} + \frac{(\gamma + 1)\left(\frac{P_s}{P_o}\right)^2}{(\gamma - 1)\left(\frac{P_s}{P_o}\right) + 2\gamma} \quad \text{Equation 1}$$

where:

- P_r = peak reflected pressure
- P_o = ambient pressure (approximately 14.7 psi)
- P_s = peak side-on pressure
- γ = ratio of specific heat (approximately 1.4)

2.2 Structural Analysis

2.2.1 SDOF Models

The dynamic responses of all structural components (i.e., roof deck, wall panels, etc.) of the MBU were calculated in accordance with the procedures in the ASCE manual *Design of Blast Resistant Buildings for Petrochemical Facilities* and Department of the Army's Technical Manual TM5-1300 *Structures to Resist the Effects of Accidental Explosions*. Using blast loads with varying peak pressures and durations, the maximum responses of the components were determined by a dynamic structural analysis. In most of the analyses, each component was modeled as an equivalent SDOF system consisting of a spring-mass system. This concept is shown in Figure 3. The equivalent SDOF system properties were determined such that the deflection of the equivalent spring-mass system would be equal to the maximum deflection of the component.

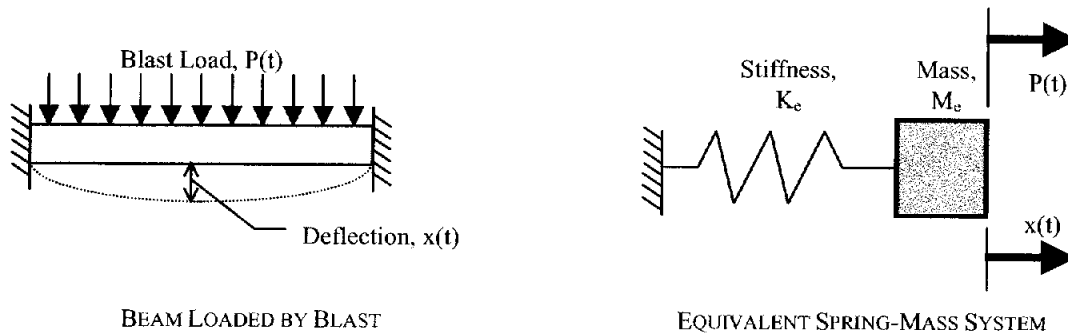


Figure 3. Equivalent Spring-Mass SDOF System

The stiffness and strength of the equivalent SDOF system springs were based on the material properties, geometry, and boundary conditions of each member. The masses of the equivalent SDOF systems were based on the weights of the components and their load-mass factors. In addition to the analysis of the individual components, the overall lateral load resisting system of the building was assessed.

The maximum deflections of the equivalent SDOF systems representing each structural component were calculated using several in-house structural analysis computer programs. These programs determine the SDOF properties and calculate the response-time history of an SDOF system for a given blast load by solving for the acceleration, velocity, and displacement at each time step based on the equation of motion. The support rotations were determined as shown in Equation 2 from the maximum calculated dynamic deflections of each component using the component span and the assumed deflected shape of the component as shown in Figure 4. The value x_m is the maximum deflection of the component over the span, L . In addition, the ductility ratios were determined. The response criteria given in Table 2 were used to determine the deflection limits for each level of damage. Note that for the crimped wall panels, an average of the response criteria of the corrugated metal panels and steel plates was used. This assumption was used because the corrugated metal panel response criteria were based in part on rib height-

to-thickness ratios ranging between 20 and 120 (typically about 50 to 100), whereas this ratio is about 19 for the crimped wall panels of the MBU. However, the crimped wall panels should have response criteria lower than that of a flat steel plate because the corrugation pattern will include stress concentrations and/or buckling not prevalent in a flat steel plate. Therefore, the response criteria used for this study were the average of the corrugated metal panel and steel plate criteria. The three damage levels (Low, Medium and High) in Table 2 are defined in detail in Table 3.

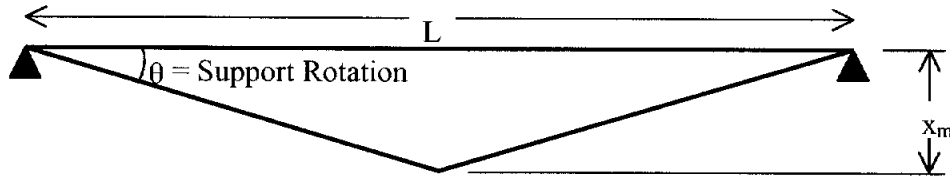


Figure 4. Illustration of Support Rotation Angle Used for Damage Criteria

$$\theta = \tan^{-1}\left(\frac{2x_m}{L}\right) \quad \text{Equation 2}$$

Table 2. Response Criteria Used to Define Damage Levels

Element Type	Upper Bound Criteria for Damage Levels					
	Low		Medium		High	
	Rotation (deg)	Ductility	Rotation (deg)	Ductility	Rotation (deg)	Ductility
Corrugated Metal Panels	1.25	1.75	2	3	4	6
Steel Plates	3	5	6	10	12	20
Crimped Wall Panels*	2	3.5	4	6.5	8	13
Steel Beams (i.e., eave struts)	2	3	6	10	12	20
Frame Sway	H/50	N/A	H/35	N/A	H/25	N/A

*Response criteria are an average of the criteria for corrugated metal panels and steel plates (not from ASCE reference).

Table 3. Component Damage Level Descriptions

Component Damage Level	Component Consequence
1 = Low	Localized component damage. Building can be used. Total cost of repairs is moderate.
2 = Medium	Widespread component damage. Building cannot be used until repaired. Total cost of repairs is significant.
3 = High	Component has lost structural integrity and may collapse due to environmental conditions (i.e., wind, snow, rain). Total cost of repairs approaches replacement cost.
4 = Failure	Complete failure of component creating debris hazard. Replacement required.

2.2.2 FEA Models

The crimped wall panels were analyzed using FEA models in addition to equivalent SDOF models since there are several interacting components that affect the panel response that an

SDOF model cannot fully capture. For example, as the crimped panel deflects, it eventually undergoes a membrane response, which transmits an in-plane reaction load to the floor and roof struts. This load causes the floor and roof struts to deflect, thereby reducing the membrane action. By using an FEA model, the crimped wall panel and the floor/roof strut can be included together.

ADINA⁴ and LS-DYNA⁵ were used for the FEA models, which are industry-accepted dynamic first-principle based codes that have the ability to compute large deformations due to flexure, shear, and instabilities such as buckling. Elastic-plastic material models were used in these analyses. Response criteria consistent with those shown in Table 2 were used for the deflection of the crimped wall panels in the FEA models. A localized failure strain of 0.20 was used as the “High Response” criteria for the crimped wall panel instead of ductility ratio; the support rotation criteria was also used.

2.2.3 Pressure-Impulse Curves

The responses of the structural components are calculated for multiple pressure-impulse (P-i) combinations to develop P-i curves representing constant magnitudes of deflection. In this manner, a P-i curve shows the pressure and impulse combinations that cause the same amount of maximum deflection and damage for a given structural component. The concept of a P-i curve is illustrated in Figure 5. All the pressure and impulse combinations defined by the curve cause the same damage level for the given structural component. The points that make up the P-i curve can be determined by using a trial-and-error method that determines the combinations of peak pressure and impulse (for a blast wave with a defined shape) that cause a specified level of response, which is further associated with a level of damage.

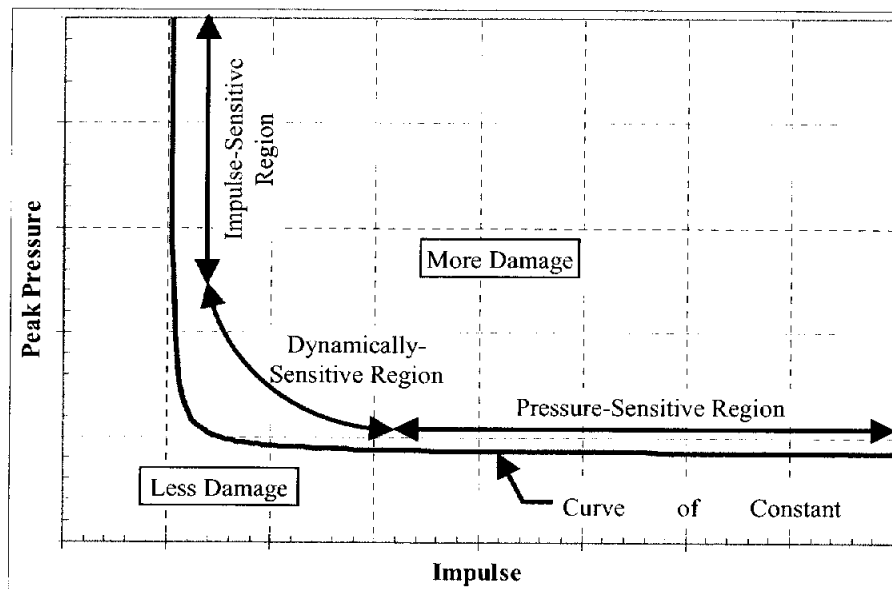


Figure 5. P-i Curve Representation

P-i curves can be used to evaluate the amount of damage in a structural member due to a given blast load. Any blast load with a pressure and impulse combination that falls below or to the left of the curve causes less damage to the component than the damage level corresponding to the P-i curve. Conversely, any blast load with a pressure and impulse falling above or to the right of the curve will cause more damage to the component. Therefore, a P-i diagram can be used to define blast loads that cause more or less than a designated damage level in the given component. Several P-i curves can be plotted on a single diagram so that the area between P-i curves can be used to define a region of approximately constant damage. In this case, all blast loads with a pressure and impulse falling within a given region of the P-i diagram will have the damage level designated for the region.

The BDLs are determined using the model presented in Table 4, which is based on the highest component damage levels (CDLs) from the two worst damaged walls and the highest CDL on the roof.

Table 4. BDL As a Function of CDL

		Roof Damage Level			
		1	2	3	4
Wall Damage Level*	1.1	1	2	2	4
	2.1	2	2	2b	4
	2.2	2	2	2	4
	3.1	2	2	2b	4
	3.2	2	2	2b	4
	3.3	2b	2b	2b	4
	4.1	2	2	2b	4
	4.2	2	2	2b	4
	4.3	2b	2b	3	4
	4.4	3	3	3	4

*Worst Damaged Wall, Second Worst Damaged Wall.
 Load bearing wall and/or frame damage level is minimum BDL.

3. STRUCTURAL ANALYSIS RESULTS

The structural analysis consisted of assessments of each component in flexural response and the overall lateral resisting system of the building.

3.1 Wall and Roof Components

3.1.1 Crimped Wall Panel

The LS-DYNA FEA mesh of the crimped wall panel is shown in Figure 6. The model consists of more than 6,000 nodes and shell elements that make up about a 1-inch grid of the tube framing and crimped wall panel. The shell elements used a $2 \times 2 \times 2$ integration scheme with Hughes-Lui integration. As seen in Figure 6, a quarter-symmetry model was used such that planes of symmetry were implemented horizontally along the midspan of the crimped wall panel (i.e., along the mid-height of the FEA model shown in Figure 6) and vertically at a location halfway between the HSS6×6× $\frac{1}{4}$ posts (i.e., a vertical plane in the middle of the FEA model shown in Figure 6). Note that the FEA model conservatively uses the HSS6×6× $\frac{1}{4}$ floor strut instead of the HSS12×6× $\frac{1}{4}$ roof strut.

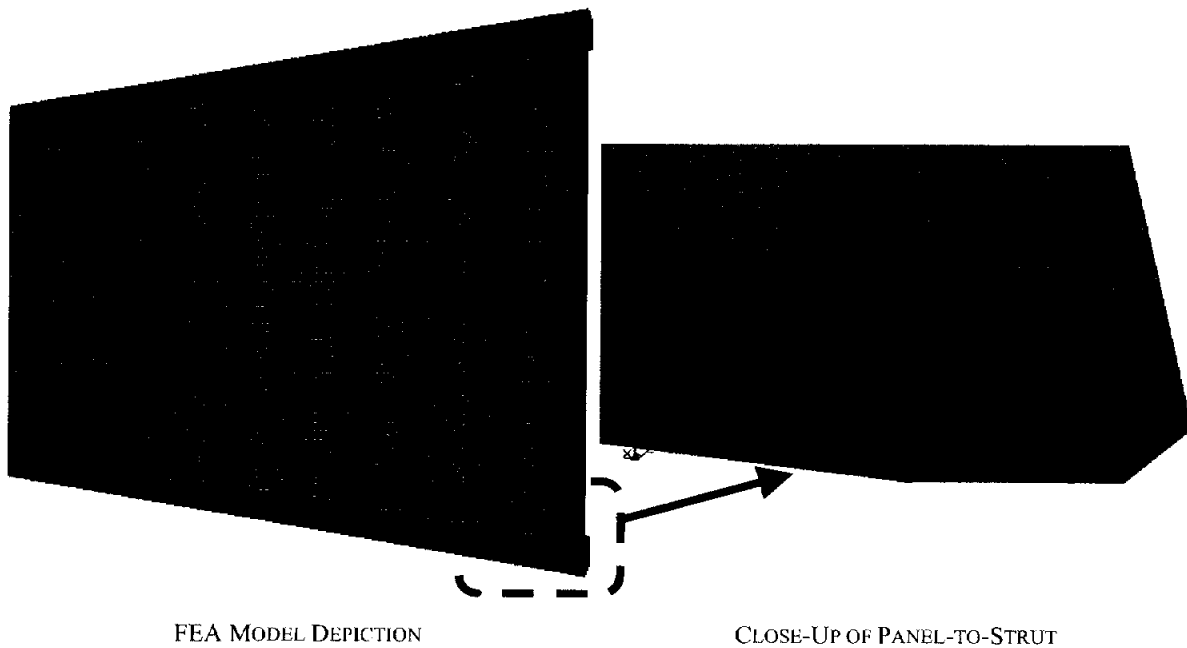


Figure 6. Crimped Wall Panel FEA Model

The crimped wall panel was modeled using ASTM A36 steel and the tube steel was modeled using ASTM A500, Grade C steel. The appropriate material modeling parameters with dynamic and material strength increase factors are included in Table 5.

Table 5. Material Properties for FEA Models

Member	f_{dv} (psi)	E (psi)	E_h (psi)	ϵ_u (%)	ν
Crimped Wall Panel	51,084	29,000,000	2,900	20	0.3
Tube Framing	57,477	29,000,000	2,900	20	0.3

As stated previously, the FEA models used planes of symmetry. A depiction of the FEA model with the appropriate boundary conditions is shown in Figure 7. Note that this figure shows the applied boundary conditions for only the one-quarter portion of the wall that was modeled. In addition to the boundary conditions used to implement planes of symmetry, the end of the floor strut (i.e., the left side of the tube) was fully fixed. Also, the top interior corner of the floor strut was pinned to prevent translation in the z-direction. This support condition is provided by the steel floor and roof plates of the building.

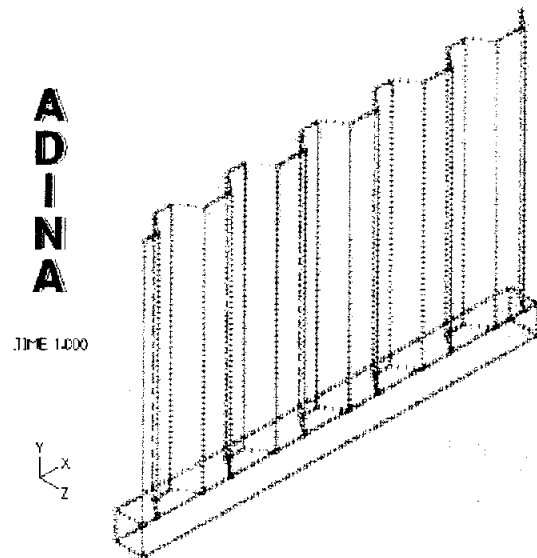


Figure 7. Model Boundary Condition Display

In addition, spring elements were included along the upper interior corner of the tubes. These springs represent the rotational stiffness provided by the C5x6.7 floor and roof joists. These spring elements are shown in Figure 8 in a view from the interior of the building.

Pressure history blast loads were applied to the ADINA finite element models in the z-direction to the entire crimped wall panel.

The results of the FEA analyses show that as the crimped wall panel deflects (i.e., in the z-direction), the supporting tube strut deflected upward. An example of the displaced shape is shown in Figure 9, along with an effective plastic strain fringe plot.

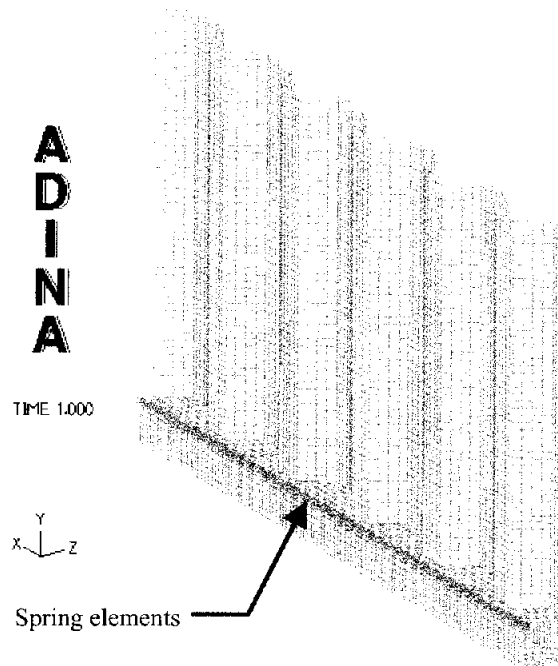


Figure 8. Interior Model View

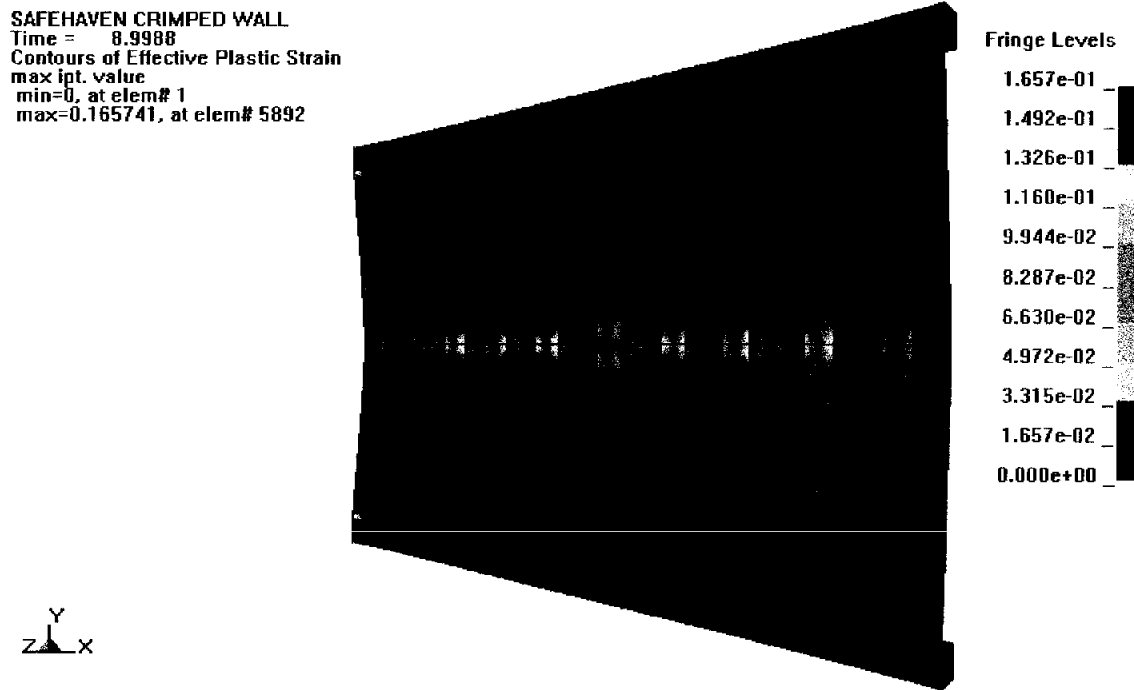


Figure 9. Crimped Panel Response for Blast Load of 40 psi and 8.75 msec

The corresponding plastic strain distribution is also shown in Figure 9. The maximum strain for this case was located in the wall panel at its end near where the tube strut is supported by the wall posts. Most of the cases considered exhibited this behavior, but a few included the maximum strain at the midspan of the wall panel.

Results of the various FEA models are shown in Figure 10 on a P-i diagram. The LS-DYNA results are labeled in terms of the peak lateral displacement for the applied blast loads. The figure also shows the P-i curves for the wall panel as determined using the SDOF method, and the P-i curves include the peak lateral displacement for each response level. As seen in the figure, the FEA results are generally in agreement with the SDOF results; therefore, the P-i curves based on the SDOF model are used for the wall panels.

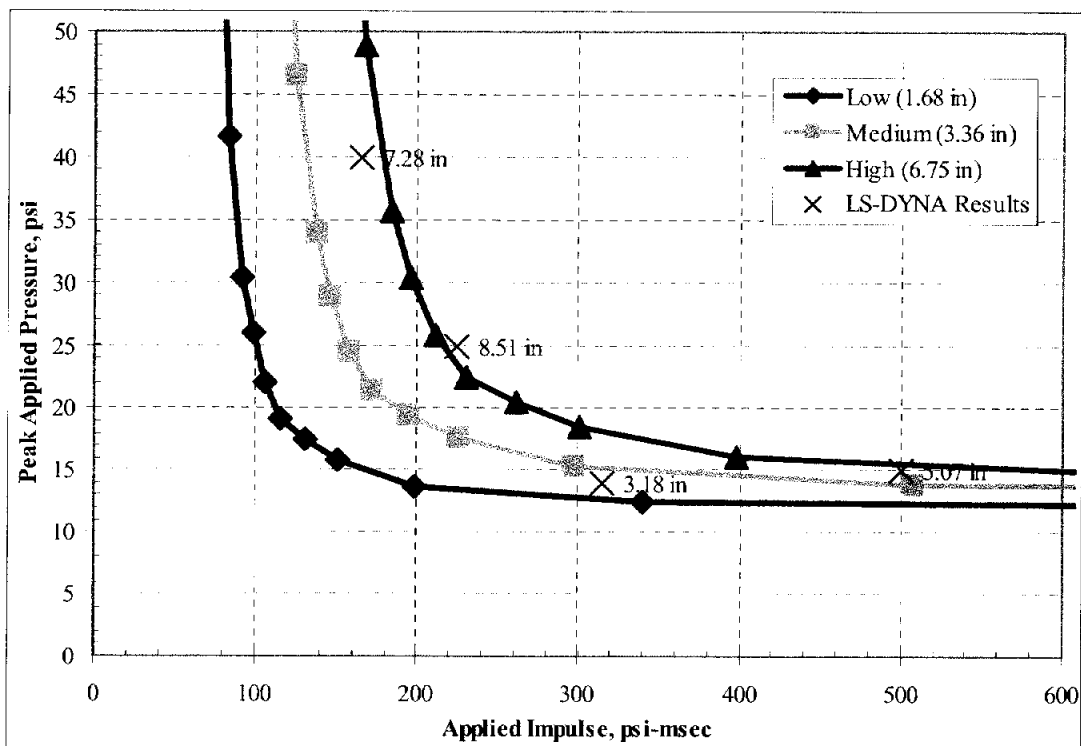


Figure 10. P-i Diagram with FEA Results for Crimped Wall Panel

3.1.2 Remaining Primary and Secondary Structural Components

The results of the structural analyses of the remaining components are shown in Table 6. These results are summarized in terms of the asymptote values of the P-i curves for each damage level for each component. The P-i curves for the controlling components along the walls and roof are shown in Figure 11. For this building, the controlling component along the walls is the crimped wall panel. The joists are the governing components for the roof for most pressure-impulse combinations. The roof plate is controlling for the impulse-sensitive region (i.e., for blast loads having pressures above 30 psi and short durations).

Table 6. Free-Field P-i Curve Asymptote Values for Structural Components

Component	Low Response		Medium Response		High Response	
	Peak Pressure (psi)	Impulse (psi-msec)	Peak Pressure (psi)	Impulse (psi-msec)	Peak Pressure (psi)	Impulse (psi-msec)
Roof Plate	13.1	47	17.3	76	19.4	105
Roof Joists	4.9	58	5.6	113	5.7	150
Eave Strut	9.5	70	10.9	135	11.2	180
Wall Panel	5.0	10	5.5	15	5.7	20
Door Posts	8.5	18	9.5	33	9.7	43

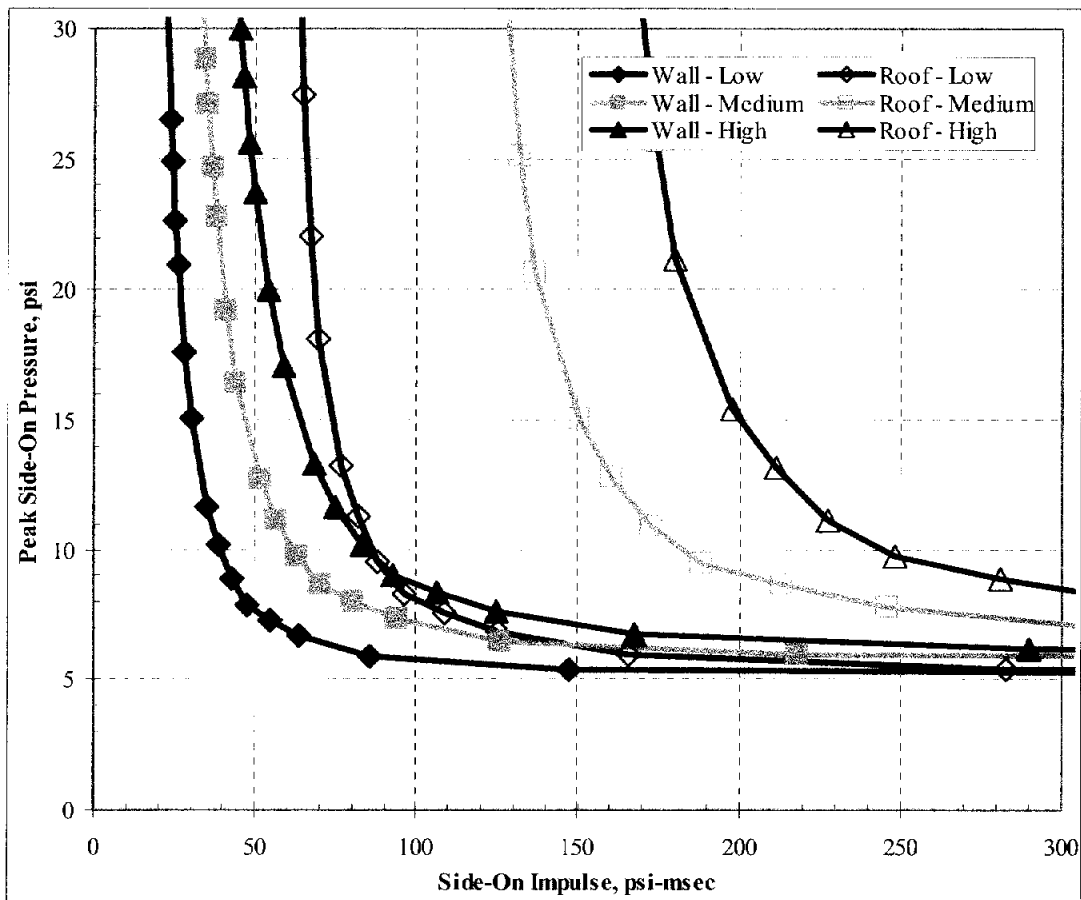


Figure 11. Controlling Wall and Roof P-i Diagram

Note that the 4-inch wall posts were evaluated for their capacity to support the end reactions of the eave struts for a vertical load. It was found that the posts' compression capacities were within 20% of the peak eave strut reactions. Since the wall panels will also serve to support the eave struts for vertically-applied loads, this was determined to be acceptable.

3.1.3 Doors and Windows

The MBU has personnel doors at both end walls (shorter 14-ft wide walls). These doors are comprised of ¼-inch steel plates sandwiching HSS1.5×1.5×¼ horizontal stiffeners. Doors are supported by a ¾-inch steel bar stock welded continuously to the door posts and headers to provide a bearing support. Each door also includes a 17-inch by 17-inch by ½-inch annealed window.

The results of the structural analyses of the door components are shown in Table 7. These results are summarized in terms of the asymptote values of the P-i curves for each damage level for each component. When comparing the values in Table 6 to Table 7, it appears that the door stiffeners are weaker than the remainder of the building. However, the door stiffener analysis included the conservative assumption that only one plate was composite with the tube. In reality, the other plate will be plug-welded from the outside and therefore will be at least partially composite, which would result in an increase in the P-i curve asymptote values for this component presented in Table 7. Therefore, the doors are considered to have no worse damage than that of the building for any given blast load.

Table 7. Free-Field P-i Curve Asymptote Values for Doors

Component	Low Response		Medium Response		High Response	
	Peak Pressure (psi)	Impulse (psi-msec)	Peak Pressure (psi)	Impulse (psi-msec)	Peak Pressure (psi)	Impulse (psi-msec)
Door Plates	7.8	11	13.9	20	22.5	34
Door Stiffener	4.7	10	5.3	17	5.4	23
Window	6.9	2.4	N/A ^a	N/A ^a	N/A ^a	N/A ^a

^aP-i diagram for window is determined only for when breakage occurs

The doors were also evaluated to determine whether they might be pushed through the doorframes. However, this was shown to not occur for the P-i curves developed. In addition, the ¾-inch bar stock was calculated to be sufficient for supporting the door.

The door should be able to withstand the blast load, but the engineering analysis does not provide a determination regarding whether it will still be operable after an explosion so that the building occupants have a means of egress from the building.

Finally, the P-i asymptote shown for the window in Table 7 includes a pressure asymptote greater than that of the building but an impulse asymptote less than the building. Thus, for blast loads having a high peak pressure and low impulse (such as for high explosives), the window is calculated to break and possibly be thrown into the building. Otherwise, the window would be predicted to remain intact for blast loads following the building P-i diagram.

It is good engineering practice to orient the building so that one of the 12-ft wide end walls faces the potential explosion source. This provides a minimum surface that would have a reflected orientation for the blast loads. Also, this would ensure that the wall with the door would not face

the potential explosion source (i.e., a side-on orientation instead of a reflected orientation) to reduce the applied blast loads for the doors.

3.2 Lateral Resisting System

The MBU design provides that the lateral resisting system consists primarily of a roof diaphragm with shear walls at the ends. There will also be some resistance provided by the moment connections between the floor/roof struts and floor/roof joists and between the floor/roof struts and columns, but these effects were conservatively ignored for the analysis of the lateral resisting system.

The worst-case loading condition for the lateral resisting system would be a long-duration blast load with a low pressure. Therefore, an equivalent static approach was used where the diaphragm and shear walls were loaded by the ultimate resistance of the wall panel. These calculations show that the lateral resisting system has a capacity greater than the ultimate resistance of the wall panel and therefore does not control the response of the building.

No details were provided to BakerRisk regarding how the MBU would be anchored to a foundation, and so no formal evaluation of sliding or overturning was completed as part of this study. However, based on our experience, this type of building tends to slide rather than overturn whether or not it is anchored to any foundation. Furthermore, even if the MBU were not anchored to a foundation, our experience indicates that it would slide only a minimal amount (on the order of a few inches). Safe Haven might consider having the effects of sliding on vulnerability of building occupants evaluated in a separate study.

3.3 Combined BDL Results

The structural analysis results were used to develop a P-i diagram for various BDLs, which is shown in Figure 12. The controlling components were the crimped wall panels, roof plate, and roof joists. The P-i curves for the wall panels corresponding to damage levels low, medium, and high represent the BDL curves for levels 1, 2b, and 3, respectively.

For this P-i diagram, the given BDL applies to the area below and to the left of the curve. For example, a blast load having a peak free-field pressure of 15 psi with a free-field impulse of 40 psi-msec would have a BDL of 2b for the MBU.

As discussed in Section 2.1, clearing effects and negative phase loading were not included in the development of the P-i diagram shown in Figure 12. These can be accounted for by using the impulse associated with these loading conditions instead of the impulse assuming a triangular shape as shown in Figure 2.

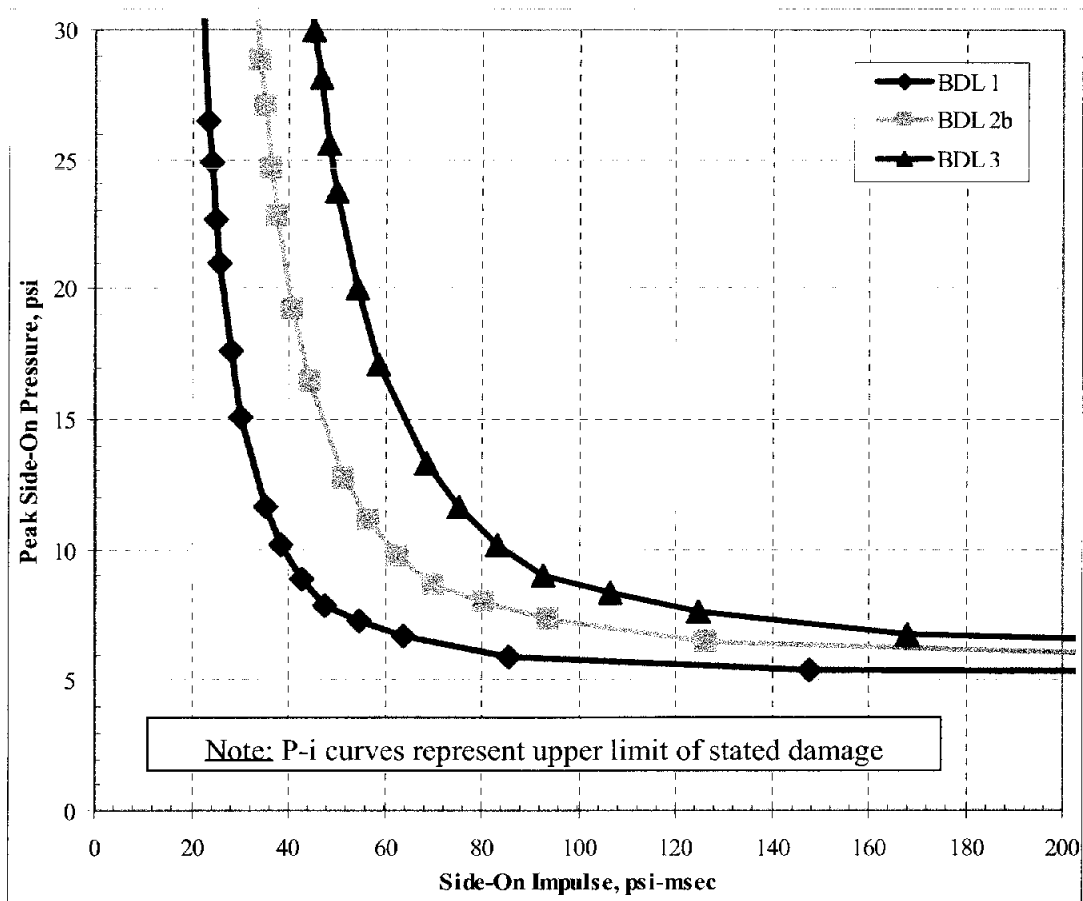


Figure 12. BDL P-i Diagram for MBU

4. CONCLUSIONS

BakerRisk has evaluated the MBU in terms of structural response to blast loads. The approach included developing P-i curves for the structural components of the building based on SDOF and FEA structural analysis models. Then, a BDL P-i diagram was determined using a combination of the component P-i curves.

The analysis completed for this study included the evaluation of all of the structural components of the building, which included the primary components (i.e., panels, joists, posts, etc.) and secondary components (i.e., diaphragms, shear walls). Items not included in the analysis included the door, anchoring system to the foundation, and sliding and overturning responses.

In general, this building has a high capacity to resist blast loads. Most high explosive threats would fall along the impulse asymptote of the building P-i diagram. In fact, it would take an exceptionally large high explosive threat to severely damage the MBU. For example, a 2,000-lb TNT charge located 140 ft away would cause a BDL of 3. In addition, a vapor cloud explosion (VCE) threat typically considered at petrochemical facilities would fall along either the pressure asymptote or within the dynamically sensitive region. It is unusual to have VCE blast loads with durations longer than 200 msec, and peak blast pressures rarely exceed 5 psi outside close proximity to a process unit. Based on the building P-i diagram, this building could be located most places in a typical petrochemical facility, including a reasonably close location to process units. However, whether this building is intended to offer protection from high explosive, VCE, or any other blast threat, its adequacy should be verified with a formal determination of the anticipated blast loads.

The controlling component for the MBU was the crimped wall panel in a primary flexural response. If desired, Safe Haven could likely increase the capacity of this building by adding more posts along the walls. These posts would provide additional support for the floor and roof struts to improve the crimped wall panel's membrane response.

It is important to note that these results represent a single MBU configuration. Additional analysis will be required for horizontally and/or vertically stacked MBU configurations. Safe Haven might also wish to consider an analysis of potential injuries to building occupants from base accelerations for MBUs not anchored to a foundation. BakerRisk can provide engineering analysis support for these considerations for Safe Haven, if desired.

5. REFERENCES

1. *Design of Blast Resistant Buildings in Petrochemical Facilities*, prepared by the Task Committee on Blast Resistant Design of the Petrochemical Committee of the Energy Division of the American Society of Civil Engineers, 1997.
2. *Structures to Resist the Effects of Accidental Explosions*, Department of the Army Technical Manual TM5-1300, Department of the Navy Publication NAVFAC P-397, Department of the Air Force Manual AFR 88-22, Revision 1, November 1990.
3. Baker, W.E., *Explosions in Air*, Wilfred Baker Engineering, San Antonio, 1983.
4. ADINA System 8.1, ADINA R&D, Inc., Watertown, MA, June 2003.
5. LS-DYNA Version 950, Livermore Software Technology Corp., Livermore, CA, May 1999.